Research article JHEP|Reports

Targeting thrombospondin-2 retards liver fibrosis by inhibiting TLR4-FAK/TGF-β signaling

Authors

Ning Zhang, Xiaoning Wu, Wen Zhang, Yameng Sun, Xuzhen Yan, Anjian Xu, Qi Han, Aiting Yang, Hong You, Wei Chen

Correspondence

cw_2011@126.com (W. Chen), youhong30@sina.com (H. You).

Graphical abstract

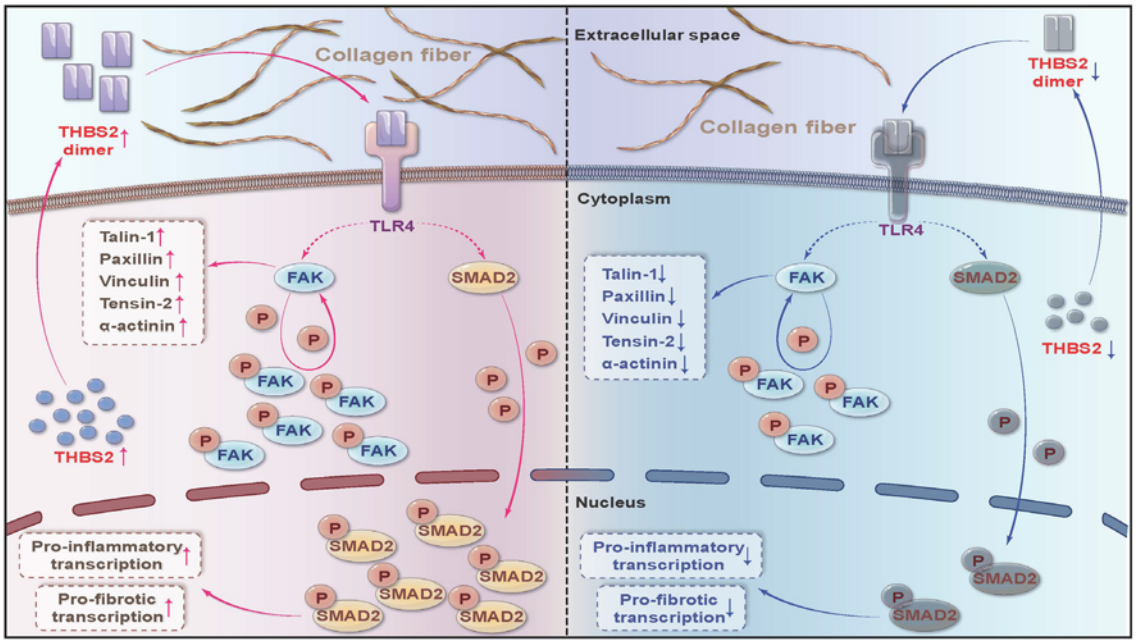

Highlights

- THBS2 expression is associated with liver fibrosis severity and decreases during fibrosis regression.
- Thbs2 inhibition in hepatic stellate cells ameliorates intrahepatic inflammation and liver fibrosis.
- Thbs2 inhibition in hepatic stellate cells suppresses metabolic dysfunction-associated steatotic liver disease progression.
- THBS2 regulates the activity of hepatic stellate cells by mediating the TLR4-TGF-β/FAK axis.
- Extracellular THBS2 directly interacts with TLR4 on hepatic stellate cells as a dimer type.

Impact and implications

Thrombospondin-2 (THBS2) is emerging as a factor closely associated with liver fibrosis regardless of etiology. However, the mechanisms by which THBS2 is involved in liver fibrosis remain unclear. Here, we showed that THBS2 plays a prominent role in the pathogenesis of liver fibrosis by activating the TLR4-TGF-β/FAK signaling axis and hepatic stellate cells in an autocrine manner, providing a potential therapeutic target for the treatment of liver fibrosis.

https://doi.org/10.1016/j.jhepr.2024.101014

Research article

JHEP|Reports

Targeting thrombospondin-2 retards liver fibrosis by inhibiting TLR4-FAK/TGF-β signaling

Ning Zhang,[1,2,3,†] **Xiaoning Wu**,[1,2,3,†] Wen Zhang,[1,2,3] Yameng Sun,[1,2,3] Xuzhen Yan,[2,3,4,5] Anjian Xu,[2,3,4,5] Qi Han,[1,2,3] Aiting Yang,[2,3,4,5] Hong You,[1,2,3,*] Wei Chen[2,3,4,5,*]

[1]*Liver Research Center, Beijing Friendship Hospital, Capital Medical University, No. 95 Yong'an Road, Xicheng District, Beijing 100050, China;* [2]*State Key Lab of Digestive Health, Beijing Friendship Hospital, Capital Medical University, No. 95 Yong'an Road, Xicheng District, Beijing 100050, China;* [3]*National Clinical Research Center of Digestive Diseases, Beijing Friendship Hospital, Capital Medical University, No. 95 Yong'an Road, Xicheng District, Beijing 100050, China;* [4]*Beijing Clinical Research Institute, Beijing Friendship Hospital, Capital Medical University, No. 95 Yong'an Road, Xicheng District, Beijing 100050, China;* [5]*Experimental and Translational Research Center, Beijing Friendship Hospital, Capital Medical University, No. 95 Yong'an Road, Xicheng District, Beijing 100050, China*

JHEP Reports **2024.** https://doi.org/10.1016/j.jhepr.2024.101014

Background & Aims: Thrombospondin-2 (THBS2) expression is associated with liver fibrosis regardless of etiology. However, the role of THBS2 in the pathogenesis of liver fibrosis has yet to be elucidated.
Methods: The *in vivo* effects of silencing *Thbs2* in hepatic stellate cells (HSCs) were examined using an adeno-associated virus vector (serotype 6, AAV6) containing short-hairpin RNAs targeting *Thbs2*, under the regulatory control of cytomegalovirus, U6 or the α-smooth muscle promoter, in mouse models of carbon tetrachloride or methionine-choline deficient (MCD) diet-induced liver fibrosis. Crosstalk between THBS2 and toll-like receptor 4 (TLR4), as well as the cascaded signaling, was systematically investigated using mouse models, primary HSCs, and human HSC cell lines.
Results: THBS2 was predominantly expressed in activated HSCs and dynamically increased with liver fibrosis progression and decreased with regression. Selective interference of *Thbs2* in HSCs retarded intrahepatic inflammatory infiltration, steatosis accumulation, and fibrosis progression following carbon tetrachloride challenge or in a dietary model of metabolic dysfunction-associated steatohepatitis. Mechanically, extracellular THBS2, as a dimer, specifically recognized and directly bound to TLR4, activating HSCs by stimulating downstream profibrotic focal adhesion kinase (FAK)/transforming growth factor beta (TGF-β) pathways. Disruption of the THBS2-TLR4-FAK/TGF-β signaling axis notably alleviated HSC activation and liver fibrosis aggravation.
Conclusions: THBS2 plays a crucial role in HSC activation and liver fibrosis progression through TLR4-FAK/TGF-β signaling in an autocrine manner, representing an attractive potential therapeutic target for liver fibrosis.
Impact and implications: Thrombospondin-2 (THBS2) is emerging as a factor closely associated with liver fibrosis regardless of etiology. However, the mechanisms by which THBS2 is involved in liver fibrosis remain unclear. Here, we showed that THBS2 plays a prominent role in the pathogenesis of liver fibrosis by activating the TLR4-TGF-β/FAK signaling axis and hepatic stellate cells in an autocrine manner, providing a potential therapeutic target for the treatment of liver fibrosis.

Introduction

Liver fibrosis is a programmed wound healing response to repeated parenchymal injury, which is characterized by excessive deposition of extracellular matrix (ECM).[1] Liver fibrosis can progress to cirrhosis, which results in more than one million deaths annually.[2] Although there is increasing evidence that suppression or elimination of prime injurious triggers brings benefits to patients, it is not always sufficient to ameliorate liver fibrosis.[3–5] Up to now, there is no approved antifibrotic therapy; thus, pharmacological drugs that specifically postpone fibrosis progression or even accelerate regression of advanced fibrosis or cirrhosis are a major unmet need.

Thrombospondin 2 (THBS2) is a disulfide-linked homotrimeric glycoprotein belonging to the thrombospondin family. Recent studies have highlighted that THBS2 may promote the formation of cancer-associated fibroblasts, orchestrating the aggressiveness of multiple cancers via stroma-cancer communications.[6–8] In intrahepatic cholangiocarcinoma, THBS2, with thrombospondin 1 and pigment epithelium-derived factor, enhances the invasiveness of carcinoma cells by facilitating lymphangiogenesis but suppressing angiogenesis.[9] Considering non-malignant liver fibrosis is the most potent risk factor for developing liver carcinogenesis, irrespective of the etiology of liver disease,[10] dysregulation patterns and the specific roles of THBS2 during liver fibrosis progression are worthy of study.

Keywords: extracellular matrix; metabolic dysfunction-associated steatohepatitis; smooth muscle α-actin promoter; myofibroblast tropism; cirrhosis.
Received 25 June 2023; received in revised form 13 December 2023; accepted 8 January 2024; available online 24 January 2024
† Co-first author.
* Corresponding authors. Address: Experimental and Translational Research Center, Beijing Friendship Hospital, Capital Medical University, No. 95 Yong'an Road, Xicheng District, Beijing 100050, China; Tel.: +86 (010) 6313-9311 (W. Chen) or +86 (010) 6313-9019 (H. You – lead contact).
E-mail addresses: cw_2011@126.com (W. Chen), youhong30@sina.com (H. You).

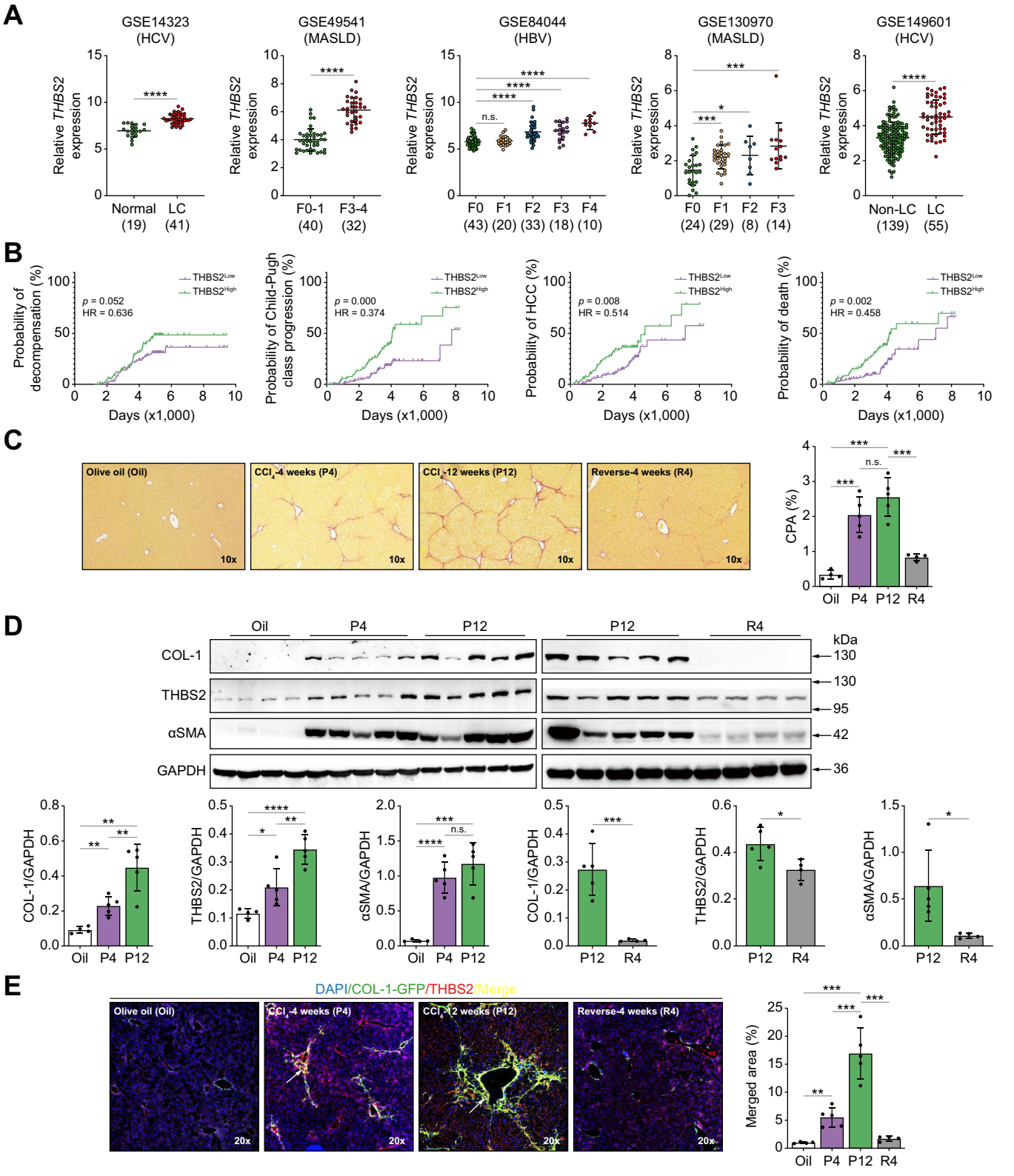

Fig. 1. THBS2 expression increases with liver fibrosis progression and decreases with regression. (A) *THBS2* gene expression in human non-fibrotic and fibrotic livers from five independent gene expression profiles retrieved from the GEO database. The sample size in each group is indicated under the corresponding scatter plot. (B) Kaplan-Meier curves of the associations between *THBS2* gene expression and the probability of decompensation occurrence, progression of Child-Pugh class, HCC onset or death in fibrotic livers from the GSE15654 dataset. *THBS2*^{Low} (n = 108) and *THBS2*^{High} (n = 108) subgroups were separated based on the mean value of *THBS2* gene expression. (C) Sirius red staining of livers from progressive and regressive fibrosis mouse models induced by CCl_4 intoxication. Objective magnification, 10x. CPA was compared among groups of mice. (D) Immunoblotting analyses of COL-1, THBS2 and αSMA protein during liver fibrosis

So far, several transcriptomic analyses have shown that the *THBS2* gene is significantly upregulated in fibrotic livers and correlated with fibrosis stages not perturbed by any etiology.[11,12] Circulating THBS2 level can stratify fibrosis severity in patients with metabolic dysfunction-associated steatohepatitis (MASH) or HCV infection, representing a promising non-invasive biomarker for liver fibrosis.[13,14] In addition, experimental mice lacking *Thbs2* exhibit frail and lax skin and connective tissues with structurally abnormal collagen fibrils, indicating that THBS2 is required for ECM homeostasis, probably by regulating ECM production, lysyl oxidase level and ECM cross-linking.[15,16] Our recent study has found that THBS2 protein is dominatingly expressed in activated hepatic stellate cells (HSCs) in the murine fibrotic liver, while targeting *THBS2* in a human HSC cell line perturbs HSC activity by affecting the intracellular Notch signaling pathway.[12] Accordingly, upregulated THBS2 in activated HSCs is likely to be involved in the pathogenesis of liver fibrosis.

To explore the role of HSC-derived THBS2 in liver fibrosis, our current study employed an adeno-associated virus serotype 6 (AAV6) vector carrying short-hairpin RNAs (shRNAs) under the regulatory control of cytomegalovirus (CMV), U6 or α-smooth muscle actin (αSMA) promoter to specifically target the *Thbs2* gene in HSCs in mouse models of carbon tetrachloride (CCl_4) or methionine-choline deficient (MCD) diet-induced liver fibrosis.

Materials and methods

Methodological details are included in the supplementary information.

Results

THBS2 expression in activated HSCs depends on liver fibrosis severity and decreases with regression

To confirm the dysregulation pattern of the *THBS2* gene in patients with liver fibrosis, five publicly available transcriptomic profiles related to liver fibrosis with different etiologies (GSE84044, GSE14323, GSE49541, GSE103580, GSE130970) were analyzed. As shown in Fig. 1A, the *THBS2* gene was evidently increased in fibrotic livers and depended on histological severity regardless of etiology. The higher expression level of the liver *THBS2* gene predicted poor prognosis in liver fibrosis (GSE15654, Fig. 1B). We next analyzed THBS2 protein expression in livers from bidirectional liver fibrosis models established based on collagen α1(I)-GFP mice under CCl_4 injury or cessation.[17] THBS2 protein that co-localized with collagen α1(I)-GFP was gradually increased along with the extension of CCl_4 administration but notably diminished as CCl_4 was withdrawn (Fig. 1C–E), and positively correlated with collagen I and αSMA expression in dynamic liver fibrosis mouse models (Fig. S2). These results indicate that THBS2 expression is associated with liver fibrosis severity and decreases during liver fibrosis regression.

Next, we analyzed the publicly available single-cell RNA sequencing dataset containing $CD45^+$ and $CD45^-$ cells from human cirrhotic and healthy livers (GSE136103).[18] As shown in Fig. S3A, activated (*LOXL1*$^+$) HSCs were the unique cellular source for *THBS2* gene expression in human cirrhotic livers. In mouse fibrotic livers, single-cell RNA sequencing analyses using Liver Cell Atlas and immunofluorescent co-localization analyses showed *Loxl1*$^+$ or $Desmin^+$ HSCs were mainly responsible for THBS2 expression; meanwhile endothelial cells ($LYVE^+$ or $CD34^+$) or Kupffer cells ($F4/80^+$) also contributed to a small proportion of THBS2 expression (Figs S3B and S4). Collectively, activated HSCs are the dominant cellular source for THBS2 expression in the fibrotic liver.

Selectively targeting *Thbs2* in HSCs ameliorates CCl_4-induced liver fibrosis progression in mice

We next tested the effects of specific inhibition of HSC *Thbs2* on liver fibrosis aggravation using an AAV6 vector carrying shRNA specifically targeting *Thbs2* under the control of the CMV promoter (Fig. S5A). Our immunostaining experiments and mRNA detection of enhanced GFP (EGFP) agreed with previous studies that AAV6 has a myofibroblast tropism[19,20] (Figs S5B and S6A). The colocalized ratio of EGFP to αSMA reached ~30-40% (Fig. S5C), indicating that the AAV6 vector has a higher myofibroblast transduction efficiency than ever reported.[19,20] AAV6-delivered shRNA achieved the expected silencing effect, as HSC THBS2 protein, total liver *Thbs2* mRNA, and serum THBS2 levels were significantly decreased in $sh^{CMV\text{-}Pr}$ compared to $NC^{CMV\text{-}Pr}$ mice (Fig. S5D–G). AAV6-shRNA delivery barely affected the liver and spleen weight of mice (Fig. S6B). Of note, it was exciting to find that *Thbs2* interference in HSCs protected against HSC activation and liver fibrosis progression in CCl_4-challenged $sh^{CMV\text{-}Pr}$ mouse models, as extracellular collagen and elastin deposition, serum alanine aminotransferase (ALT) level, and intrahepatic collagen I, THBS2, elastin and αSMA protein were evidently reduced in $sh^{CMV\text{-}Pr}$ mice compared to $NC^{CMV\text{-}Pr}$ mice following CCl_4 treatment (Fig. S5H–J). Fluorescence-activated cell sorting combined with gene quantitation analyses further confirmed that *Thbs2*, *Acta2*, and *Col1a1* were significantly downregulated in $CD45^-Desmin^+$ HSCs isolated from $sh^{CMV\text{-}Pr}$ compared to $NC^{CMV\text{-}Pr}$ mice (Fig. S7).

We repeated the above experiments using AAV6-U6-sh*Thbs2*-EGFP ($sh^{U6\text{-}Pr}$) with a different shRNA targeting HSC *Thbs2* under the control of the U6 promoter. As expected, we achieved consistent results in $sh^{CMV\text{-}Pr}$ mouse models (Figs S8 and S9). In addition, Rezvani *et al.* found that AAV6 also transduced a small proportion of Kupffer cells.[19] As we found THBS2 was also slightly expressed in intrahepatic macrophages and endothelial cells, we replaced the CMV promoter – that usually induces strong expression and has compatibility with numerous cell types – in our AAV6 delivery system with the αSMA promoter to specifically target *Thbs2* in HSCs (Fig. 2A). We demonstrated that the αSMA promoter in the AAV6 delivery system exhibited comparable efficiency as CMV or U6 promoters and hardly affected the liver and spleen weight of mice (Fig. 2B–G and

progressive and regressive mouse models injured by CCl_4. (E) Immunofluorescent staining of THBS2 and visualization of COL-1-GFP in fibrosis progressive and regressive mouse liver slices. Objective magnification, 20x. The yellow color in the merged images illustrates the co-localization of COL-1 (green) and THBS2 (red). Merge area percentage was calculated and compared among groups. Data are presented as the mean ± SEM (n = 4-5/group). Statistical evaluation was performed using one-way ANOVA followed by Tukey's multiple comparisons test among three or more groups or using Student's *t* test between two groups (*p <0.05; **p <0.01; ***p <0.001; ****p <0.0001). CCl_4, carbon tetrachloride; CPA, collagen proportionate area; HCC, hepatocellular carcinoma; HR, hazard ratio; LC, cirrhosis; MASLD, metabolic dysfunction-associated steatotic liver disease; non-LC, non-cirrhosis; n.s., not significant.

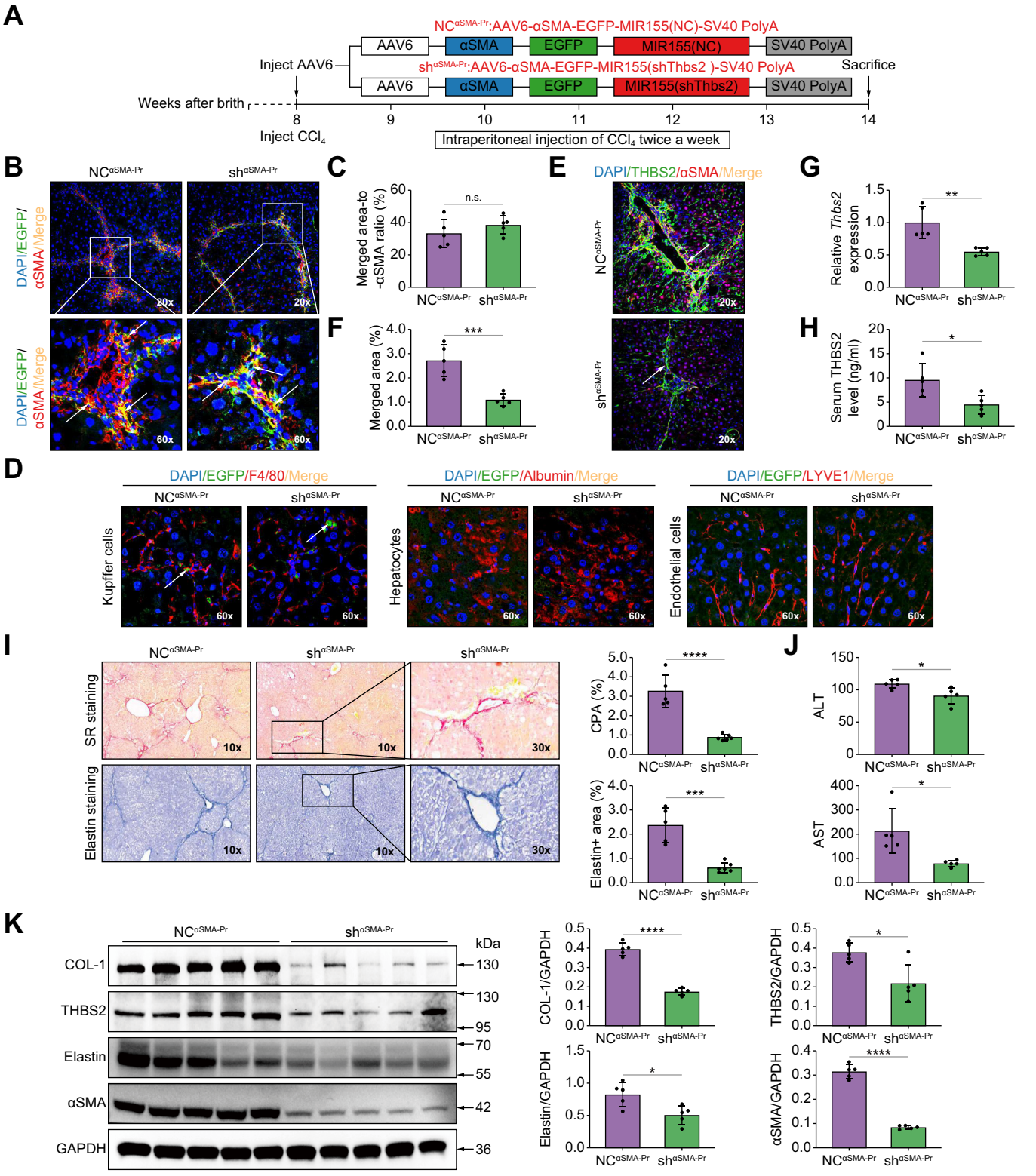

Fig. 2. Selective inhibition of *Thbs2* in HSCs by AAV6-αSMA-sh*Thbs2*-EGFP vector ameliorates CCl_4-induced liver fibrosis in mice. (A) Schematic diagram of time points for AAV6 vector injection, CCl_4 administration and sacrifice of mice. (B) Immunofluorescent staining of EGFP and αSMA in liver slices from AAV6-αSMA–NC–EGFP ($NC^{αSMA-Pr}$) and AAV6-αSMA-sh*Thbs2*-EGFP ($sh^{αSMA-Pr}$) groups of mice. Objective magnification, 20x and 60x. Co-localization of EGFP (green) and αSMA (red) is shown as yellow. (C) The merged area (yellow) of the EGFP (green) to αSMA (red) ratio was calculated and compared between groups. (D) Immunofluorescent staining of THBS2 (green), F4/80 (red), Albumin (red), LYVE1 (red), and CD34 (red) in liver slices from mice with CCl_4-induced liver fibrosis. The merged areas are shown in yellow. Objective magnification, 60x. (E) Co-localization (yellow) of THBS2 (green) and αSMA (red) in liver slices from $NC^{αSMA-Pr}$ and $sh^{αSMA-Pr}$ mice. Objective magnification, 20x. (F) Co-localized area (yellow) percentage was calculated and compared between groups. (G) Comparison of liver *Thbs2* gene expression between $NC^{αSMA-Pr}$ and $sh^{αSMA-Pr}$ mice. (H) Comparison of serum THBS2 level between $NC^{αSMA-Pr}$ and $sh^{αSMA-Pr}$ mice. (I) SR and elastin

Fig. S10). Immunofluorescent staining showed AAV6 with an αSMA promoter mainly transduced into αSMA$^+$ HSCs, slightly targeted F4/80$^+$ Kupffer cells, and hardly infected Albumin$^+$ hepatocytes and LYVE$^+$ endothelial cells (Fig. 2B and H), indicating that AAV6 with an αSMA promoter has strong tropism for activated HSCs. Compared to NC$^{\alpha SMA\text{-}Pr}$ mice, sh$^{\alpha SMA\text{-}Pr}$ mice showed an evident decrease in ECM structural protein accumulation, serum ALT and aspartate aminotransferase levels, and liver collagen I, elastin and αSMA protein expression (Fig. 2I–K). Taken together, targeting *Thbs2* in HSCs protects against HSC activation and CCl_4-induced liver fibrosis progression.

AAV6-sh*Thbs2* delivery in HSCs relieves intrahepatic inflammation stimulated by long-term CCl_4 injury in mice

Besides fibrosis, we also observed that AAV6-sh*Thbs2* delivery under the control of the CMV promoter significantly reduced the histologic inflammatory foci and lobular necrosis (Fig. 3A). Further staining of F4/80, CD68, and CK19 and transcriptional quantification of proinflammatory cytokines (*Il1b*, *Il6* and *Tnf*) confirmed the reduction in intrahepatic inflammation after chronic CCl_4 intoxication in sh$^{CMV\text{-}Pr}$ mice compared to NC$^{CMV\text{-}Pr}$ mice (Fig. 3B and C). Because NF-κB is a crucial transcription factor modulating the expression of these proinflammatory genes and acting as a central link between intrahepatic inflammation and fibrosis,[21] we measured the expression changes of hepatic NF-κB units. As shown in Fig. 3D, liver p65 (one of the five members of the NF-κB family), phosphorylated p65, IκBα and phosphorylated IκBα were evidently decreased, indicating a weakened activation of NF-κB/IκBα signaling in response to HSC *Thbs2* inhibition by AAV6-sh*Thbs2* delivery. Co-immunofluorescent staining of THBS2 and F4/80 further confirmed that the AAV6 vector transduced a small proportion of Kupffer cells, as a noticeable reduction of THBS2 in resident macrophages from sh$^{CMV\text{-}Pr}$ mice was observed (Fig. 3E).

Likewise, by using the sh$^{U6\text{-}Pr}$ system as aforementioned, we successfully validated the robustness of *Thbs2* knockdown in relieving intrahepatic inflammation induced by CCl_4 injury (Fig. S11). Previous studies have shown that activated HSCs can secret various inflammatory molecules to activate infiltrating macrophages;[22] therefore, we inferred that specifically targeting *Thbs2* in HSCs could prevent HSC activation, thus reducing inflammation. When the CMV promoter was replaced with the αSMA promoter in the AAV6-sh*Thbs2* delivery system, THBS2 protein was still present in F4/80$^+$ macrophages but showed a slight decrease in sh$^{\alpha SMA\text{-}Pr}$ compared to NC$^{\alpha SMA\text{-}Pr}$ mice (Fig. 3F). As expected, histologic inflammation, Kupffer cell activation (F4/80$^+$ and CD68$^+$), ductular reaction (CK19$^+$), expression of proinflammatory genes (*Il1b*, *Il6*, *Tnf* and *Ccl2*) and hepatic NF-κB/IκBα signaling activation were significantly diminished in sh$^{\alpha SMA\text{-}Pr}$ mice (Fig. 3G–J), suggesting a selective inhibition of HSC *Thbs2* also reduces chronic CCl_4 administration-induced hepatitis.

Crosstalk of HSC *Thbs2* and fibrogenic TGF-β/FAK signaling perturbs HSC activation

Previous studies have shown that canonical fibrogenic transforming growth factor-β (TGF-β) and focal adhesion kinase (FAK) signaling are downstream effectors of THBS2 in tumors .[8,23] Hence, we examined whether HSC *Thbs2* knockdown hampers their activation during liver fibrosis progression. First, TGF-β signaling was found to be inhibited as its markers, including TGF-β, TGFβR2, YKL-40, and p-SMAD2/3 to SMAD2/3 ratio, were notably decreased in total livers from both sh$^{CMV\text{-}Pr}$ and sh$^{\alpha SMA\text{-}Pr}$ mice compared to corresponding control mice (Fig. 4A). Immunofluorescent staining revealed total and nuclear p-SMAD2/3 was significantly reduced in αSMA$^+$ HSCs from sh$^{CMV\text{-}Pr}$ and sh$^{\alpha SMA\text{-}Pr}$ mice (Fig. 4B), implying a deactivation of TGF-β signaling in HSCs. Inhibition of *THBS2* gene expression by small-interfering RNA or lentiviral particle-coated sh*THBS2* transfection or THBS2 peptide incubation in LX-2 cells and human primary HSCs perturbed TGF-β signaling and HSC activation (Fig S12A and B and Fig. 4C), further confirming that THBS2 influences HSC activation by regulating TGF-β signaling. Second, immunoblotting of FAK, p-FAK, Talin-1, Tensin-2, Vinculin, α-Actinin, and Paxillin demonstrated that FAK signaling was also suppressed in total livers from mice injected with AAV6-sh*Thbs2* vector under the control of CMV or αSMA promoters (Fig. 4D). In addition, cytoplasmic p-FAK was reduced in αSMA$^+$ HSCs from sh$^{CMV\text{-}Pr}$ and sh$^{\alpha SMA\text{-}Pr}$ mice (Fig. 4E), indicating inhibition of FAK signaling in HSCs. Similarly, *THBS2* inhibition or THBS2 peptide treatment in LX-2 cells and human primary HSCs perturbed FAK signaling and HSC activation (Fig. S12C and D and Fig. 4F).

We next verified the specificity of the THBS2 stimulatory effect on TGF-β/FAK signaling and subsequent HSC activation using THBS2 peptide, TGF-β signaling inhibitor (LY2157299), and FAK signaling inhibitor (PF-562271) in LX-2 cells. THBS2 peptide treatment increased collagen I, αSMA, p-SMAD2 and p-FAK expression, while the effects were abolished by pre-incubation with LY2157299 or PF-562271 (Fig. 4G and H). These results suggest that THBS2 regulates HSC activation specifically via crosstalk with TGF-β/FAK signaling and its inhibition prevents TGF-β/FAK signaling-mediated HSC activation.

TLR4 bridges extracellular THBS2 and intracellular TGF-β/FAK signaling axis in HSC activation

Given THBS2 is a secreted protein, we thereby hypothesized it would execute biological functions by acting on plasma membrane receptors. Via IPA (Ingenuity Pathway Analysis) software, we identified the potent downstream effectors of THBS2, among which toll-like receptor 4 (TLR4) is a membrane protein (Fig. 5A) and has been previously reported to interact with THBS2 in colorectal cancer cells;[24] meanwhile, TGF-β/FAK signaling is the downstream effector of TLR4.[25,26] Hence, we speculated TLR4 would act as the bridge linking extracellular THBS2 and the intracellular TGF-β/FAK signaling axis in HSC activation. As shown in Fig. S13, TLR4 protein expression was also associated with fibrosis severity and was positively correlated with THBS2. Besides, liver TLR4 protein was significantly decreased in total livers, Kupffer cells, and activated HSCs in response to specific inhibition of HSC *Thbs2* (Fig. 5B–D). Most importantly, the co-localization of THBS2 and TLR4 in non-parenchymal cells almost disappeared after HSC *Thbs2* inhibition (Fig. 5E).

staining of liver slices from NC$^{\alpha SMA\text{-}Pr}$ and sh$^{\alpha SMA\text{-}Pr}$ mice. Objective magnification, 10x and 30x. CPA or elastin positive area was compared between the two groups. (J) Serum ALT and AST levels between NC$^{\alpha SMA\text{-}Pr}$ and sh$^{\alpha SMA\text{-}Pr}$ mice. (K) Immunoblotting analyses of liver COL-1, THBS2, elastin (tropoelastin), and αSMA proteins in NC$^{\alpha SMA\text{-}Pr}$ and sh$^{\alpha SMA\text{-}Pr}$ mice. Data are presented as the mean ± SEM (n = 5/group). Statistical evaluation was performed using student's *t* test (*p <0.05; **p <0.01; ***p <0.001; ****p <0.0001). AAV6, adeno-associated virus serotype 6; ALT, alanine aminotransferase; AST, aspartate aminotransferase; CPA, collagen proportionate area; EGFP, enhanced GFP; NC, negative control; n.s., not significant; sh, short-hairpin; SR, Sirius red.

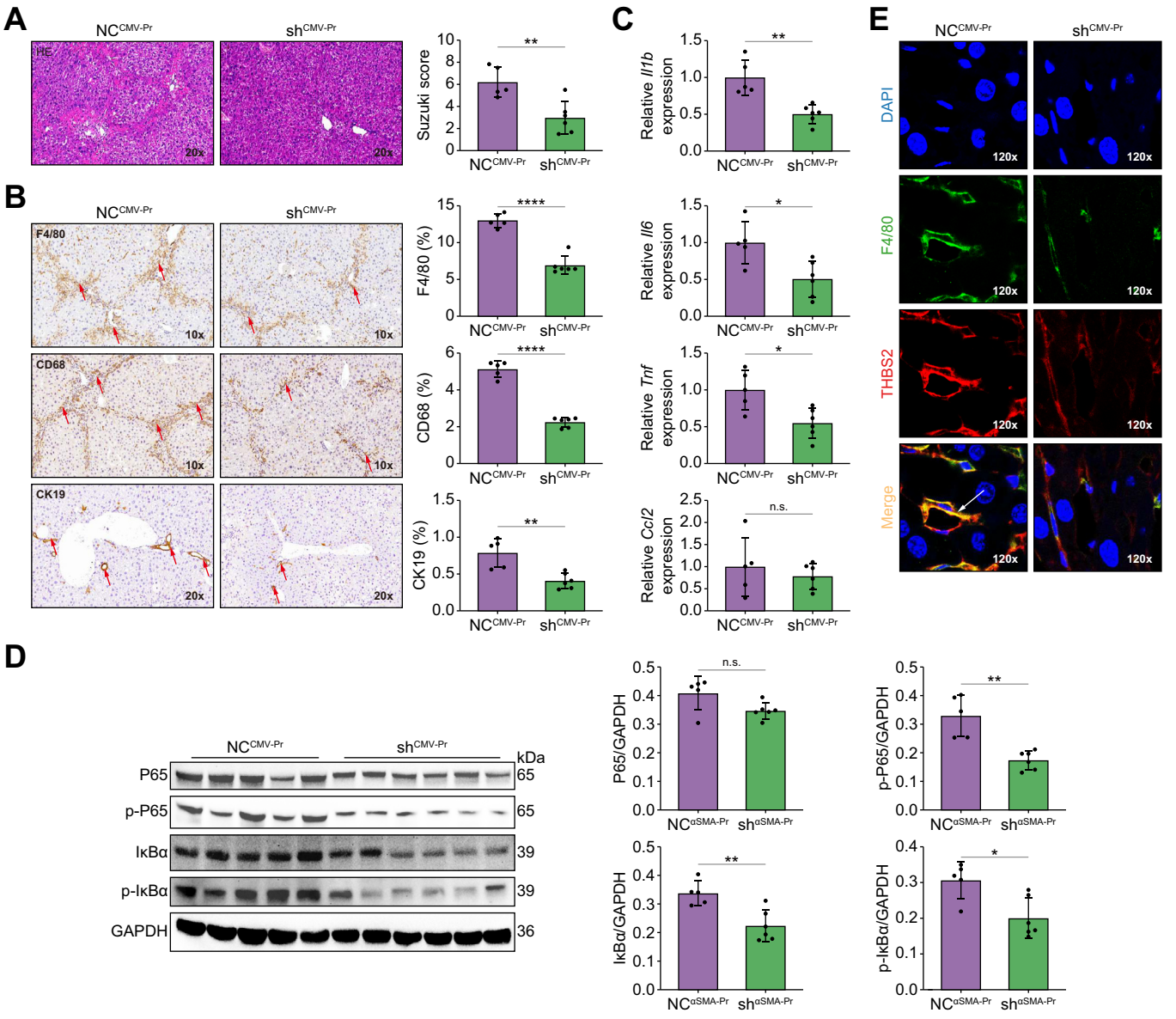

Fig. 3. AAV6-sh*Thbs2* delivery in HSCs relieves intrahepatic inflammation induced by long-term CCl_4 injury. (A) H&E staining of liver slices from $NC^{CMV\text{-}Pr}$ and $sh^{CMV\text{-}Pr}$ mice and comparison of Suzuki scores. Objective magnification, 20x. (B) Immunohistochemical staining of F4/80, CD68 and CK19 in liver slices from $NC^{CMV\text{-}Pr}$ and $sh^{CMV\text{-}Pr}$ mice and comparison of positive areas. Objective magnification, 10x and 20x. (C) Liver proinflammatory gene expression measurement and comparison between $NC^{CMV\text{-}Pr}$ and $sh^{CMV\text{-}Pr}$ mice. (D) Immunoblotting analyses of liver NF-κB units in $NC^{CMV\text{-}Pr}$ and $sh^{CMV\text{-}Pr}$ mice. (E) Co-localization (yellow) of F4/80 (green) and THBS2 (red) in liver slices from $NC^{CMV\text{-}Pr}$ and $sh^{CMV\text{-}Pr}$ mice. Objective magnification, 120x. (F) Co-localization (yellow) of F4/80 (green) and THBS2 (red) in liver slices from $NC^{\alpha SMA\text{-}Pr}$ and $sh^{\alpha SMA\text{-}Pr}$ mice. Objective magnification, 120x. (G) H&E staining of liver slices from $NC^{\alpha SMA\text{-}Pr}$ and $sh^{\alpha SMA\text{-}Pr}$ mice and comparison of Suzuki scores. Objective magnification, 20x. (H) Immunohistochemical staining and comparison of F4/80, CD68, and CK19 in liver slices from $NC^{\alpha SMA\text{-}Pr}$ and $sh^{\alpha SMA\text{-}Pr}$ mice. Objective magnification, 10x and 20x. (I) Liver proinflammatory gene expression measurement and comparison between $NC^{\alpha SMA\text{-}Pr}$ and $sh^{\alpha SMA\text{-}Pr}$ mice. (J) Immunoblotting analyses of liver NF-κB units in $NC^{\alpha SMA\text{-}Pr}$ and $sh^{\alpha SMA\text{-}Pr}$ mice. Data are presented as the mean ± SEM (n = 5-6/group). Statistical evaluation was performed using student's *t* test (**p* <0.05; ***p* <0.01, ****p* <0.001, *****p* <0.0001). AAV6, adeno-associated virus serotype 6; CCl_4, carbon tetrachloride; HSC, hepatic stellate cell; NC, negative control; n.s., not significant; sh, short-hairpin.

Accordingly, we conclude a close relationship exists between THBS2 and TLR4 in HSCs.

Next, we tested the effect of THBS2 on TLR4-TGF-β/FAK signaling and HSC activation using LX-2 cells. As shown in Fig. 5F and G, THBS2 peptide increased THBS2, TLR4, TGF-β signaling (p-SMAD2), FAK signaling (p-FAK) and HSC activation (collagen I and αSMA) in a concentration- and time-dependent manner. The specificity of the stimulatory effect of THBS2 peptide-TLR4 crosstalk was determined using a TLR4 inhibitor (TAK-242); co-incubation of TAK-242 significantly counteracted THBS2 peptide-mediated activation of TGF-β/FAK signaling and HSCs (Fig. 5H). Furthermore, *THBS2* plasmid-transfection could also induce intracellular TLR4-TGF-β/FAK signaling in LX-2 cells, which was blocked specifically by pre-incubation with a TLR4

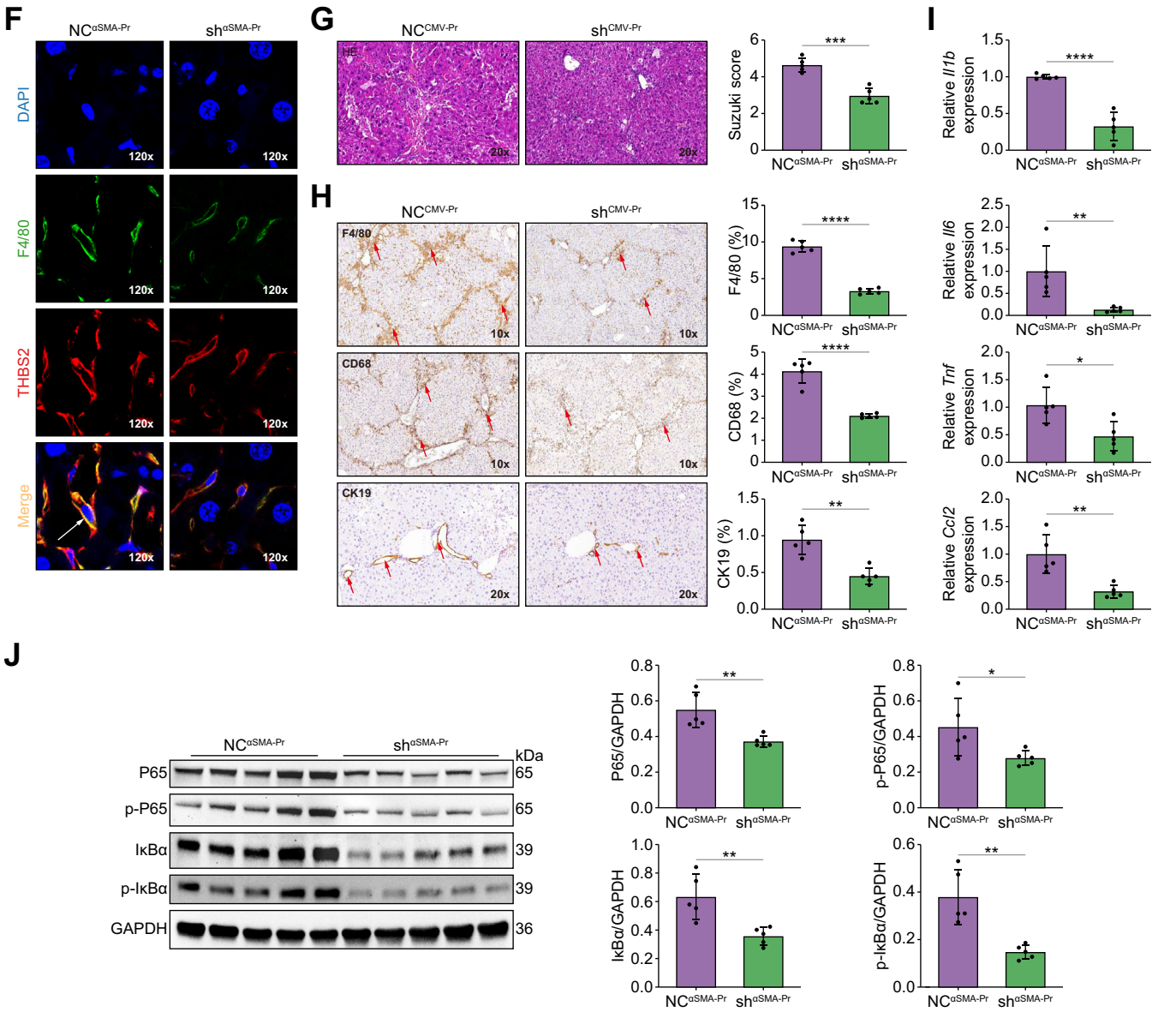

Fig. 3 (*continued*).

inhibitor (Fig. S14). Taken together, we conclude that TLR4 is the mediator responsible for THBS2-induced TGF-β/FAK signaling and HSC activation.

Extracellular THBS2 directly interacts with TLR4 on HSCs as a dimer type

To affirm how THBS2 communicates with TLR4 in HSCs, we first studied the co-localization of THBS2 and TLR4 in human primary HSCs and LX-2 cells grown in conditioned media from LX-2 cells after *THBS2* overexpression. As shown in Fig. 6A and B, we observed a robust positive co-localization of THBS2 and TLR4 at the cell surface membranes of both primary HSCs and LX-2 cells, indicating intracellular THBS2 is translocated to the ECM, with the potential to interact with TLR4 on HSCs. Next, we performed the co-immunoprecipitation study using HEK293T cells to determine whether there is a physical interaction between THBS2 and TLR4. TLR4 was co-immunoprecipitated with THBS2 after THBS2 overexpression, the interaction of which was *THBS2* plasmid dose-dependent; *vice versa*, THBS2 was also co-immunoprecipitated with TLR4 in a *TLR4* plasmid dose-dependent manner (Fig. 6C). Next, we aimed to determine whether THBS2 interacts with TLR4 in a direct way. Far-western blotting was performed using human recombinant (rh)THBS2 and rhTLR4 proteins. As shown in Fig. 6D, the far-western blotting assay confirmed the direct interaction between THBS2 and TLR4. Interestingly, we also observed the molecular weight of intracellular THBS2 was less than 130 kDa, while the molecular weight of THBS2 binding to TLR4 and the rhTHBS2 was ~250 kDa (Fig. 6C and D). Given this, we inferred that extracellular THBS2 is likely to be presented as a dimer. Therefore, we compared THBS2 protein from cell lysates and conditioned media from LX-2 cells with *THBS2* overexpression by immunoblotting. The results confirmed our assumption (Fig. 6E). In summary, intracellular THBS2 is secreted into the ECM space, as a dimer type,

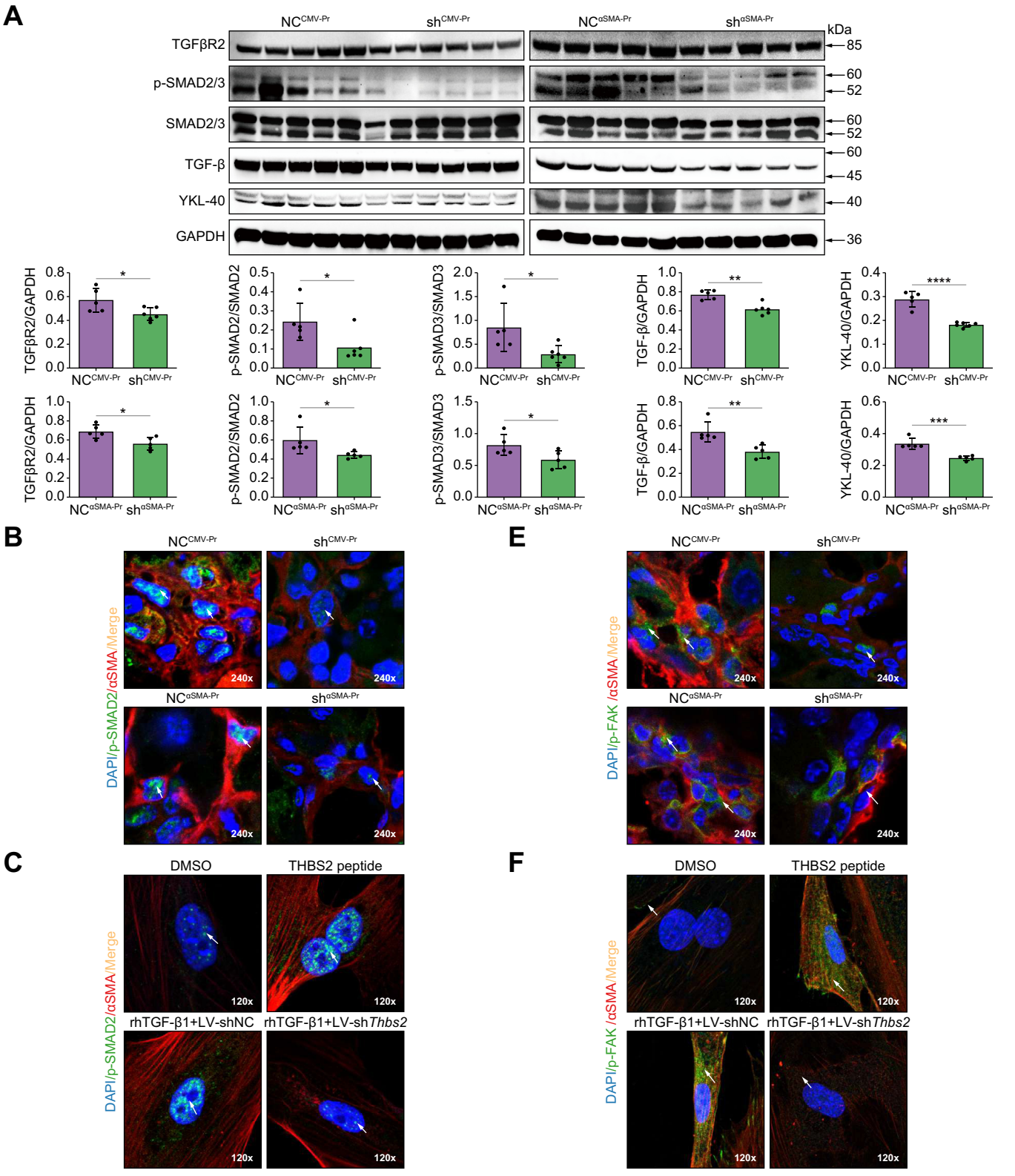

Fig. 4. THBS2 perturbs downstream TGF-β/FAK signaling and subsequent HSC activity. (A) Immunoblotting analyses of TGF-β signaling markers in livers from $NC^{CMV\text{-}Pr}$, $sh^{CMV\text{-}Pr}$, $NC^{\alpha SMA\text{-}Pr}$, and $sh^{\alpha SMA\text{-}Pr}$ mice. Ratios of p-SMAD2/SMAD2 and p-SMAD3/SMAD3 were calculated. (B) Immunofluorescent staining of p-SMAD2 (green) and αSMA (red) in liver slices from $NC^{CMV\text{-}Pr}$, $sh^{CMV\text{-}Pr}$, $NC^{\alpha SMA\text{-}Pr}$, and $sh^{\alpha SMA\text{-}Pr}$ mice. Objective magnification, 240x. (C) Immunofluorescent staining of p-SMAD2 (green) and αSMA (red) in human primary HSCs treated with DMSO, THBS2 peptide dissolved in DMSO (1 μg/ml, 24 h), rhTGF-β1 (10 μg/ml, 24 h) plus lentiviral particle (LV)-shNC (5.0×10^7 TU/ml, 72 h), and rhTGF-β1 (10 μg/ml, 24 h) plus LV-sh*THBS2* (5.0×10^7 TU/ml, 72 h). Objective magnification, 120x. (D) Immunoblotting analyses of FAK signaling markers in livers from $NC^{CMV\text{-}Pr}$, $sh^{CMV\text{-}Pr}$, $NC^{\alpha SMA\text{-}Pr}$ and $sh^{\alpha SMA\text{-}Pr}$ mice. The ratio of p-FAK/FAK was calculated. (E) Immunofluorescent staining of p-FAK (green) and αSMA (red) in liver slices from $NC^{CMV\text{-}Pr}$, $sh^{CMV\text{-}Pr}$, $NC^{\alpha SMA\text{-}Pr}$, and $sh^{\alpha SMA\text{-}Pr}$ mice. Objective magnification, 240x. (F) Immunofluorescent staining of p-FAK (green) and αSMA (red) in human primary HSCs treated with DMSO, THBS2 peptide dissolved in DMSO (1 μg/ml, 24 h), rhTGF-β1 (10 μg/ml, 24 h) plus LV-shNC (5.0×10^7 TU/ml, 72 h), and rhTGF-β1 (10 μg/ml, 24 h) plus LV-sh*THBS2* (5.0×10^7 TU/ml, 72 h). Objective magnification,

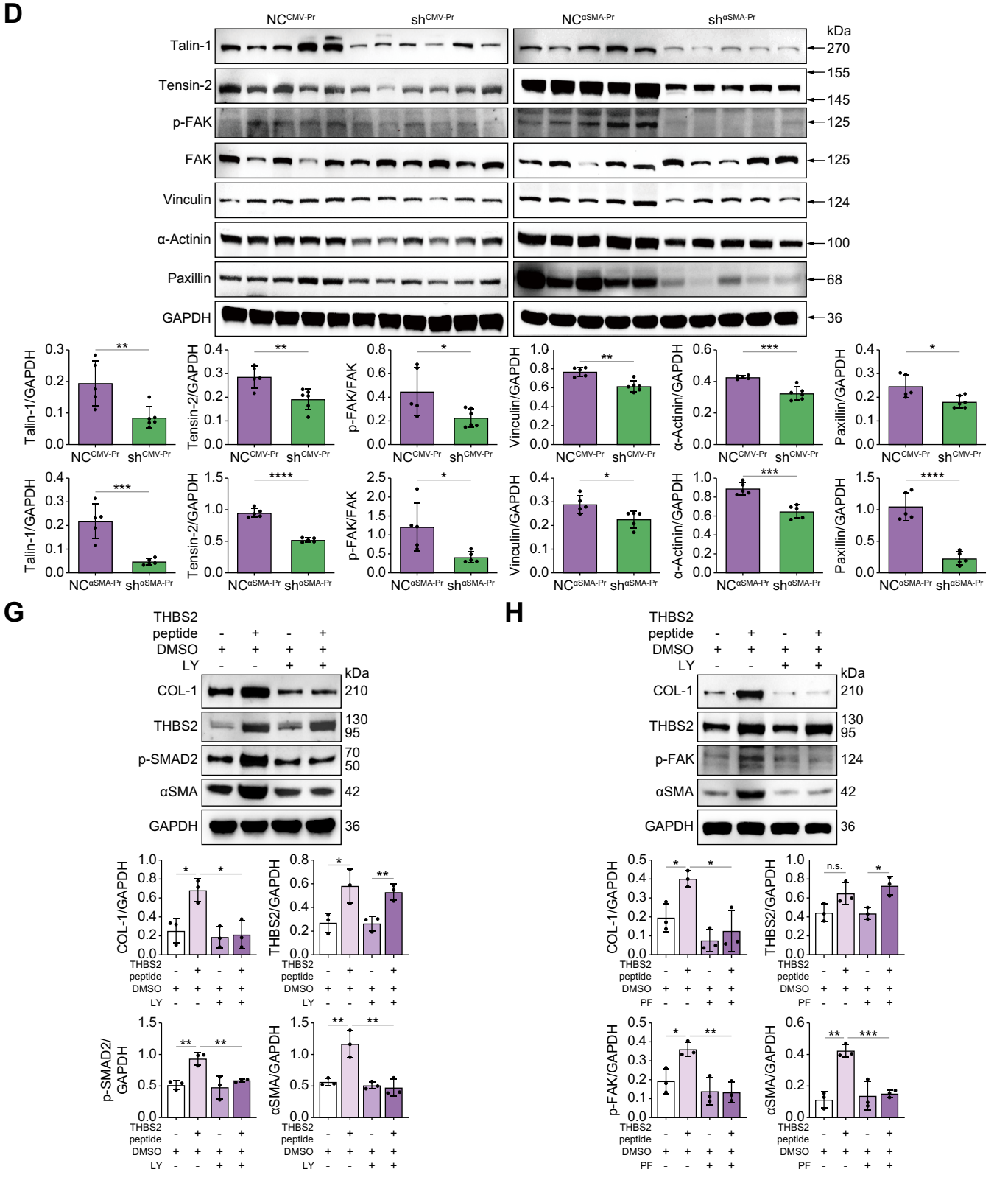

Fig. 4 (*continued*).

120x. (G) Effects of THBS2 peptide (1 μg/ml, 24 h) and/or TGF-β signaling inhibitor (LY2157299 [LY], 1 μM, 24 h) treatment on COL-1, THBS2, p-SMAD2, and αSMA expression in LX-2 cells. (H) Effects of THBS2 peptide (1 μg/ml, 24 h) and/or FAK signaling inhibitor (PF-562271 [PF], 1 μM, 24 h) treatment on COL-1, THBS2, p-FAK, and αSMA expression in LX-2 cells. Data are presented as the mean ± SEM (n = 5-6/group mice; n = 3/group cells). Statistical evaluation was performed using one-way ANOVA followed by Tukey's multiple comparisons test among three or more groups or using Student's *t* test between two groups (**p* <0.05; ***p* <0.01; ****p* <0.001; *****p* <0.0001). HSC, hepatic stellate cell; NC, negative control; n.s., not significant; rh, recombinant human; sh, short-hairpin.

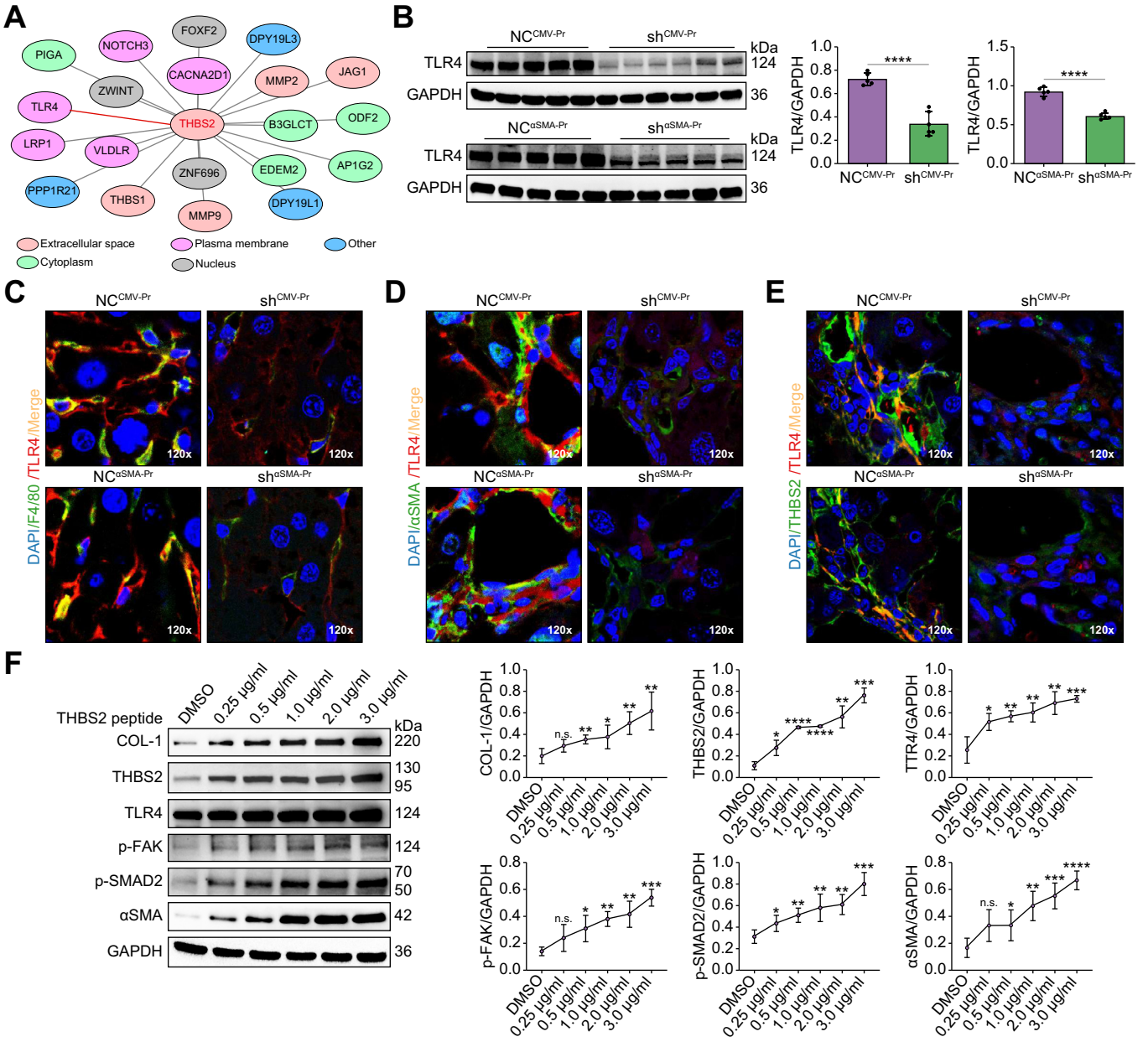

Fig. 5. THBS2 regulates the TLR4-TGF-β/FAK signaling axis and mediates HSC activation. (A) Network (visualized by Cytoscape software) of THBS2 and its potential downstream effectors (retrieved by IPA software). A node represents a protein/gene, and an edge represents a potential interaction. Different subcellular members are color-coded. (B) Immunoblotting analyses of TLR4 in livers from NC^{CMV-Pr}, sh^{CMV-Pr}, NC$^{αSMA-Pr}$, and sh$^{αSMA-Pr}$ mice. Immunofluorescence co-localization analyses of (C) TLR4 (red) and F4/80 (green), (D) TLR4 (red) and αSMA (green), or (E) TLR4 (red) and THBS2 (green) in liver slices from NC^{CMV-Pr}, sh^{CMV-Pr}, NC$^{αSMA-Pr}$ and sh$^{αSMA-Pr}$ mice. Objective magnification, 120x. Immunoblotting analyses of COL-1, THBS2, TLR4, p-FAK, p-SMAD2, and αSMA in response to (F) varying concentrations (0.25-3 μg/ml, 24 h) of THBS2 peptide treatment and (G) varying durations (0-48 h) of incubation with THBS2 peptide (1 μg/ml) in LX-2 cells (n = 3 for each group). (H) Effects of THBS2 peptide (1 μg/ml, 24 h) and/or TLR4 inhibitor (TAK-242 [TAK], 1 μM, 24 h) treatment on COL-1, THBS2, TLR4, p-FAK, p-SMAD2 and αSMA expression in LX-2 cells. Data are presented as the mean ± SEM (n = 5/group mice; n = 3/group cells). Statistical evaluation was performed using one-way ANOVA followed by Tukey's multiple comparisons test among three or more groups or using Student's *t* test between two groups (**p* <0.05; ***p* <0.01; ****p* <0.001; *****p* <0.0001). HSC, hepatic stellate cell; NC, negative control; n.s., not significant; sh, short-hairpin.

where it directly interacts with TLR4 on HSCs and amplifies biochemical signals in an autocrine manner.

AAV6-sh*Thbs2* delivery in HSCs inhibits MASH progression and liver TLR4-FAK/TGF-β pathway

Given serum THBS2 has been reported as a promising non-invasive biomarker for MASH,[13] we finally tested the effects of AAV6-sh*Thbs2* delivery in HSCs on MASH progression using MCD diet-fed mouse models (Fig. 7A). As shown in Fig. 7B–G and Fig. S15A–C, the AAV6-sh*Thbs2* vector with an αSMA promoter specifically transduced sinusoidal αSMA^{+} HSCs, reduced serum THBS2 levels and intrahepatic *Thbs2* mRNA expression, improved the tolerance to glucose loading, decreased serum triglyceride and total cholesterol contents, slightly affected serum ALT and aspartate aminotransferase levels, but had no effect on liver and spleen weights. Histologically, sh$^{αSMA-Pr}$ showed milder intrahepatic steatosis,

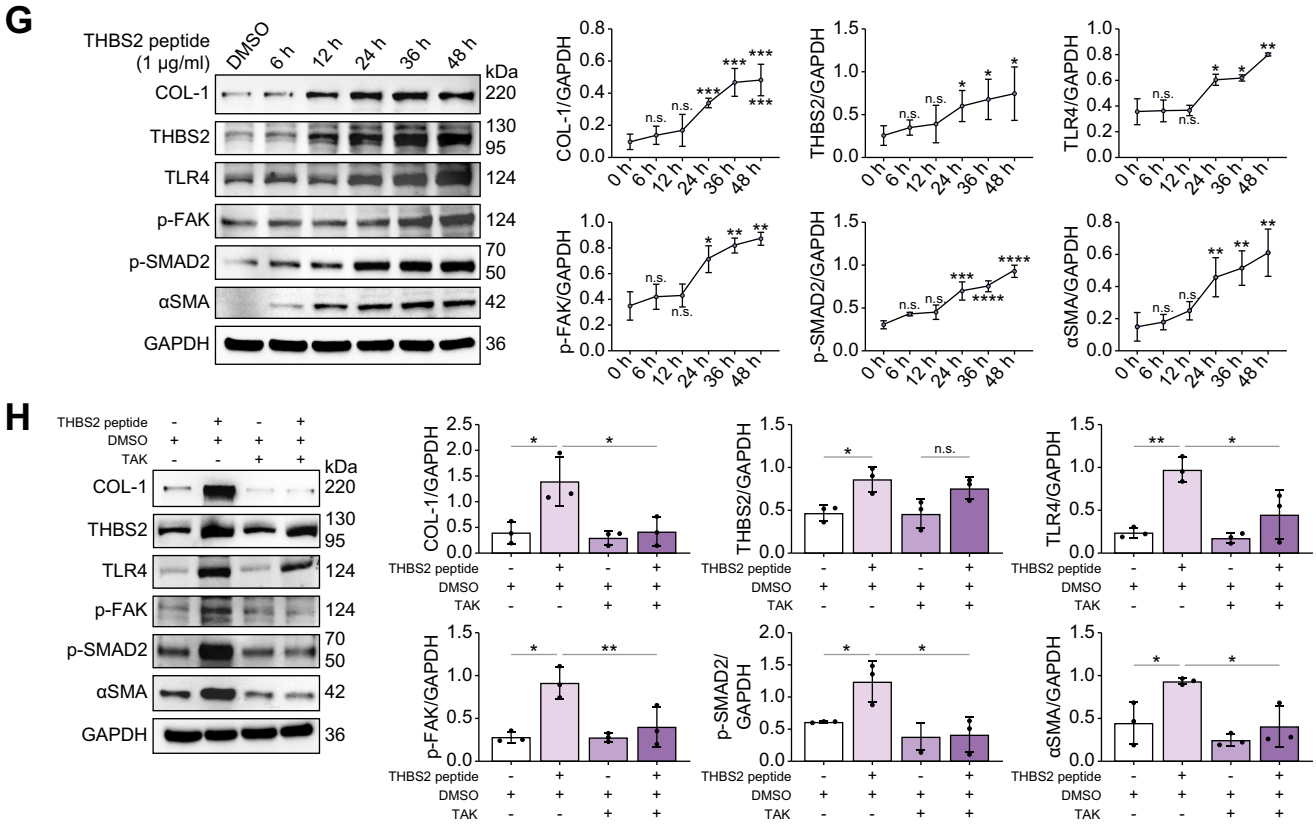

Fig. 5 (*continued*).

inflammation, and fibrosis compared to NC$^{\alpha SMA\text{-}Pr}$ mice in response to a 6-week MCD diet (Fig. 7H). At the molecular level, expression of fatty acid synthesis or transport genes (*Acc1*, *Fas*. *Screbf1* and *Cd36*) and proinflammatory genes (*Il1b* and *Il6*) was significantly downregulated in sh$^{\alpha SMA\text{-}Pr}$ compared to NC$^{\alpha SMA\text{-}Pr}$ mice fed the MCD diet (Fig. 7I and J). Moreover, compared to controls, injection of the AAV6-sh*Thbs2* vector with an αSMA promoter also reduced liver THBS2, COL-1, αSMA, TLR4, p-FAK and p-SMAD2 protein expression after a 6-week MCD diet (Fig. 7K). Collectively, specific inhibition of *Thbs2* in HSCs can attenuate TLR4-FAK/TGF-β signaling and MASH progression.

Discussion

Activation of HSCs into proliferative, contractile, and matrix-producing myofibroblasts in response to various liver injuries remains a dominant pathogenesis driving liver fibrosis progression and amplifying immunoregulation.[1,22] A clearer understanding of targets that facilitate or restrain HSC activation will contribute to guiding the development of antifibrotic therapies. In a previous study, we found that THBS2 protein is mainly upregulated in activated HSCs in the murine fibrotic liver and human HSC cell lines in response to rhTGF-β1 stimulation.[12] Besides, other studies have confirmed the value of serum THBS2 levels in diagnosing liver fibrosis .[13,14,27] These findings suggest a close relationship between upregulated THBS2 and liver fibrosis. However, the role of HSC-specific THBS2 in liver fibrosis has not been elucidated yet. Our current study demonstrates that THBS2 expression levels in activated HSCs are associated with fibrosis severity and decrease during fibrosis regression. THBS2 is principally produced and secreted from HSCs into the extracellular space, forming a dimer and directly binding to TLR4 and stimulating downstream profibrotic TGF-β/FAK signaling-mediated HSC activation; most importantly, specifically targeting *Thbs2* in HSCs using a AAV6-sh*Thbs2* delivery system retards HSC activation, ECM accumulation, and inflammatory infiltration in CCl_4 mouse models and attenuates MASH progression in mice fed a MCD diet. Our study unveils the pathogenic underpinning of THBS2 in HSC activation and liver fibrosis, providing the rationale for potential therapeutic targeting.

As well known, TGF-β/SMAD signaling is a canonical pathway responsible for activating HSCs and transdifferentiating them into myofibroblasts;[28] specific blockade of TGF-β1 signaling has been demonstrated to induce the remission of liver fibrosis in various animal models.[29] Our present study found specific inhibition of HSC *THBS2* deactivates TGF-β1-SMAD2/3 signaling *in vivo* and *in vitro*; *vice versa*, THBS2 peptide treatment activates this profibrotic signaling in HSCs, suggesting THBS2 may act as an upstream regulator of TGF-β1-SMAD2/3 signaling. The specificity of the effect of THBS2 on TGF-β signaling activation was validated through THBS2 peptide stimulation, in a dose- or time-dependent manner, as well as with the TGF-β signaling inhibitor LY 2157299. Nan *et al.* recently reported that TGF-β1 and THBS2 also constitute a complex feedback circuit activating mitogen-activated protein kinase signaling in reciprocal interactions between cancer cells and cancer-associated fibroblasts, indicating TGF-β signaling may also stimulate THBS2 expression.[8] In HSCs, the crosstalk between THBS2 and TGF-β signaling may enhance cell activation and lead to the production of various inflammatory molecules or activation of Kupffer cells in a paracrine manner, which to some extent explains the prominent inhibition

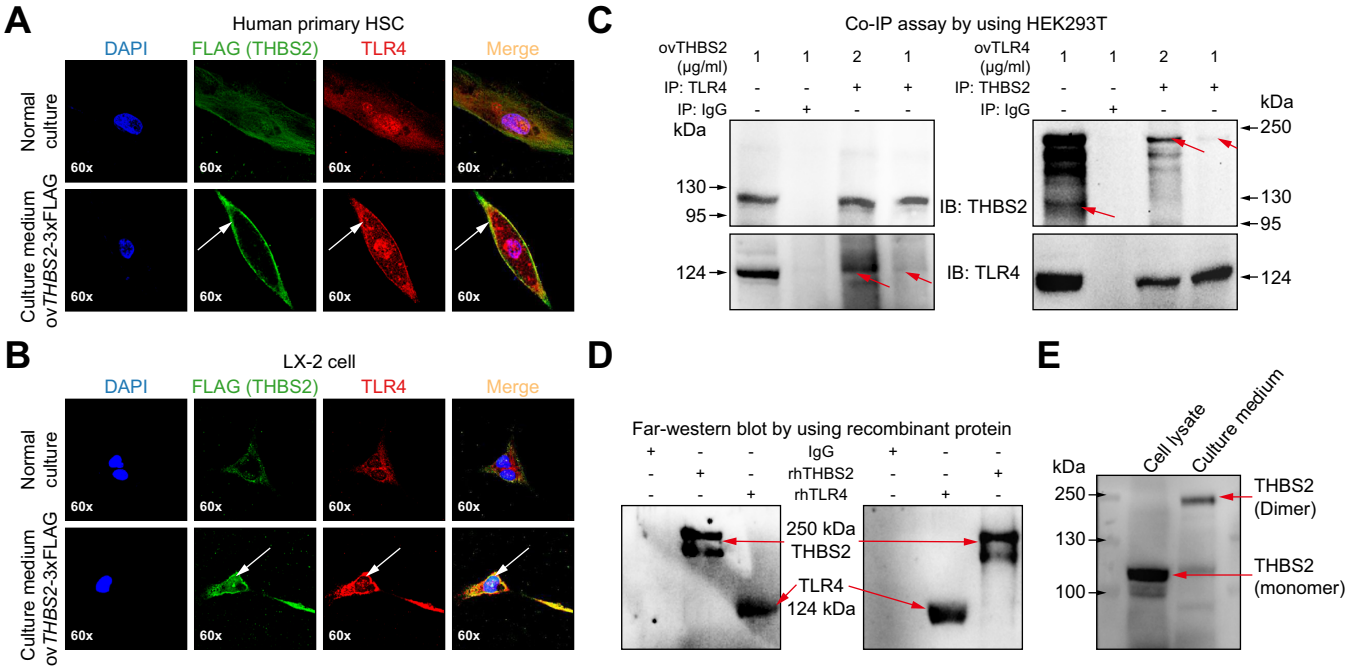

Fig. 6. Co-localization and co-IP of THBS2 and TLR4. Immunofluorescent co-localization analyses of TLR4 and FLAG (THBS2) in (A) human primary HSCs with or without incubation (72 h) of conditioned media from *THBS2*-FLAG plasmid-transfected LX-2 cells (1 μg/ml, 48 h), and (B) LX-2 cells with or without incubation (72 h) of conditioned media from *THBS2*-FLAG plasmid-transfected LX-2 cells (1 μg/ml, 48 h). The co-localized area on the cell plasma membrane is marked by the white arrow. Objective magnification, 60x. (C) Co-IP of THBS2 and TLR4 in HEK293T cells after *THBS2* overexpression (1-2 μg/ml, 48 h) or *TLR4* overexpression (1-2 μg/ml, 48 h). After *THBS2* overexpression, whole cell lysates were subjected to IP with anti-TLR4 antibody or IgG; immunoprecipitated complexes were analyzed by immunoblotting of both THBS2 and TLR4. After *TLR4* overexpression, whole cell lysates were subjected to IP with anti-THBS2 antibody or IgG; immunoblotting of both THBS2 and TLR4 analyzed immunoprecipitated complexes. IP experiments were repeated three times. (D) Far-western blotting of THBS2-TLR4 complex in HEK293T cells using rhTHBS2 and rhTLR4 proteins. Equal amounts (500 ng) of IgG, rhTHBS2, and rhTLR4 were translocated to nitrocellulose membranes following SDS-PAGE. Nitrocellulose membranes were incubated with rhTHBS2 or rhTLR4 (1 μg) for 2 h and then visualized with anti-THBS2 or anti-TLR4 antibody. Far-western blotting experiments were repeated three times. (E) Immunoblotting analyses of THBS2 from LX-2 cell lysates (overexpressing *THBS2*) and conditioned media from LX-2 cells (overexpressing *THBS2*). The experiments were repeated three times. IP, immunoprecipitation; rh, recombinant human.

of intrahepatic inflammatory infiltration after HSC *Thbs2* knockdown *in vivo*. Apart from TGF-β signaling, our recent studies have highlighted that FAK signaling is one of the specific pathways involved in liver fibrosis regardless of etiology.[12,30] Also, FAK has been experimentally confirmed to play an essential role in HSC activation and liver fibrosis progression.[31] Interestingly, THBS2 has been predicted to be involved in FAK signaling in previous studies.[12,32] Our present study experimentally demonstrates that the perturbation of THBS2 expression also specifically modulates downstream FAK signaling and HSC activity *in vivo* and *in vitro*.[12]

Next, IPA software (QIAGEN, CA, USA) analysis, together with previous studies, show LRP1,[33] NOTCH3,[33] VLDLR, CACNA2D1,[34] TLR4[24] and integrin αvβ3/CD36[8] are specific cell receptors for the THBS2 ligand. Among these receptors, TLR4 has been linked to downstream TGF-β/FAK signaling.[25,26] In addition, TLR4 is highly localized on HSCs and dynamically upregulated during liver fibrosis progression, while its inhibition has been shown to prevent TGF-β/FAK signaling and subsequent HSC activation. An early study shows TLR4 activation in HSCs sensitizes them to TGF-β signals and thus allows for unrestricted activation by Kupffer cells in liver fibrosis.[25] In cancer cells, THBS2 has been found to interact with TLR4 but not with other toll-like receptors.[24] Given this, we tried to verify whether TLR4 is a specific receptor for secreted THBS2 in HSCs. Our present study, using immunofluorescent co-localization, co-immunoprecipitation coupled with far-western blotting, has confirmed that THBS2 directly binds to TLR4 on the membrane of HSCs. Moreover, liver TLR4 expression is positively associated with THBS2 and is diminished along with specifically targeting *Thbs2* in HSCs *in vivo*. The functional roles of THBS2-TLR4 crosstalk on downstream TGF-β/FAK signaling and HSC activation were validated using THBS2 peptide, *THBS2* plasmid, and/or a TLR4-specific inhibitor in HSCs. More interestingly, extracellular THBS2 acts on TLR4 as a dimer form, as the molecular weight of THBS2 located in the ECM is nearly two-fold higher than that of intracellular THBS2. However, the regulatory mechanisms involved in the formation of THBS2 dimers and whether obstruction of such dimer formation will relieve liver fibrosis are worthy of investigation.

Currently, growing evidence from animal models highlights that AAV-dependent gene therapy has therapeutic potential for liver fibrosis via the correction of aberrantly dysregulated liver fibrosis-causing genes at the molecular level.[35] In this study, we used AAV6 carrying specific shRNAs targeting *Thbs2* in HSCs to examine whether and how THBS2 acts on liver fibrosis, since among the commonly used AAVs, only AAV6 shows a relevant myofibroblast tropism.[19] Of note, AAV6 has been successfully tested in hepatic reprogramming of activated HSCs *in vivo* by carrying hepatic transcription factors and specifically targeting *Nestin*$^{+}$ HSCs by sh*Nestin* delivery in fibrotic mouse models.[19,20] By using AAV6 carrying two independent shRNAs specically

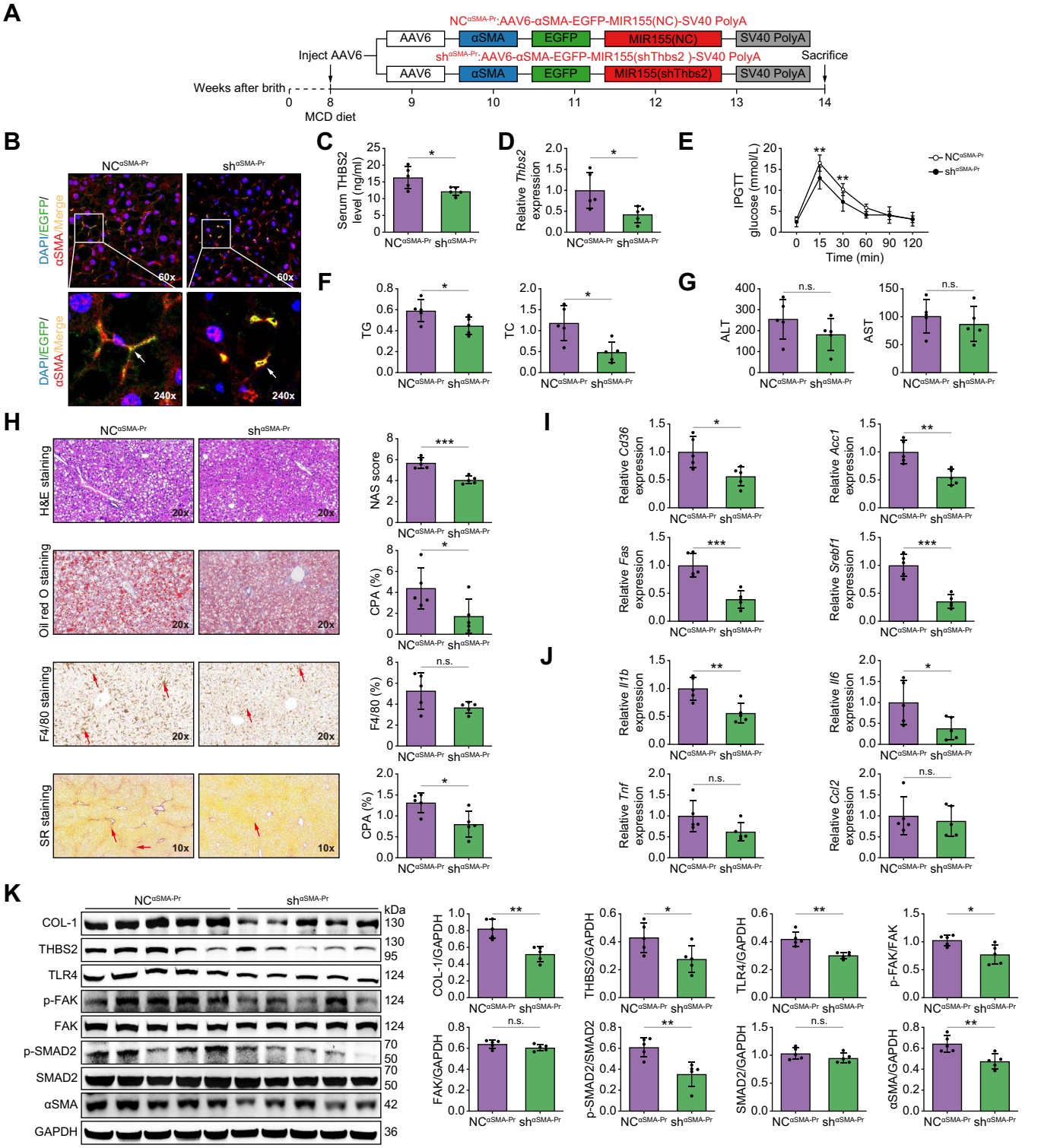

Fig. 7. AAV6-sh*Thbs2* delivery in HSCs reduces intrahepatic steatosis, inflammation, and fibrosis and inhibits liver TLR4-FAK/TGF-β pathway in mice fed the MCD diet. (A) Schematic diagram of time points for AAV6 vector injection, MCD diet, and sacrifice of mice. (B) Immunofluorescent staining of EGFP (green) and αSMA (red) in liver slices from NC$^{αSMA-Pr}$ and sh$^{αSMA-Pr}$ mice fed the MCD diet. Objective magnification, 20x and 60x. Co-localization of EGFP (green) and αSMA (red) is shown as yellow. (C) Comparison of serum THBS2 level between NC$^{αSMA-Pr}$ and sh$^{αSMA-Pr}$ mice fed the MCD diet. (D) Comparison of liver *Thbs2* gene expressions between NC$^{αSMA-Pr}$ and sh$^{αSMA-Pr}$ mice. (E) IPGTT. AAV6-sh*Thbs2* (αSMA promoter) delivery in HSCs significantly improved glucose tolerance at 25 and 30 min. Values displayed are means ± SEM of 5 mice per group. (F) Comparisons of serum TG and TC levels between NC$^{αSMA-Pr}$ and sh$^{αSMA-Pr}$ mice fed the MCD diet. (G) Comparisons of serum ALT and AST levels between NC$^{αSMA-Pr}$ and sh$^{αSMA-Pr}$ mice fed the MCD diet. (H) H&E, Oil Red O, F4/80 and SR staining of liver slices from NC$^{αSMA-Pr}$ and sh$^{αSMA-Pr}$ mice fed the MCD diet. Objective magnification, 10x and 20x. NAS score, Oil Red O-positive area, F4/80-positive area, and CPA were compared between two groups. (I,J) Measurements and comparisons of fatty acid synthesis and transport gene expression or proinflammatory gene expression

targeting *Thbs2* under the control of CMV or U6 promoters, we demonstrated that HSC-specific *Thbs2* inhibition *in vivo* effectively protects against HSC activation, ECM deposition, and inflammatory infiltration in fibrotic mouse models. In this study and a previous study by Rezvani *et al.*,[19] it was shown that the AAV6 vector mainly infects HSCs but also infects Kupffer cells to a lesser degree. As the addition of cell-specific promoters to the genome of AAVs can help regulate target gene expression in specific cells and thus improve therapeutic efficacy (for example, hepatocyte-specific thyroxin binding globulin promoter in the AAV8-shRNA delivery system),[36] we replaced the CMV promoter with the activated HSC-specific αSMA promoter[37,38] in the AAV6-sh*Thbs2* delivery system and further confirmed the therapeutic value of targeting *Thbs2*. Our AAV6-sh*Thbs2* delivery system under the control of CMV, U6, or αSMA promoters has a higher transduction efficiency in αSMA$^+$ HSCs (∼30-40%) than ever reported (∼10-20%),[19,20] although the totally injected viral genomes of the AAV6 vector are comparable. In addition, as previously reported,[19,20] intravenous injection of the AAV6 vector scarcely affects liver histology, liver weight or spleen weight.

In conclusion, our current study has demonstrated that selective silencing of *Thbs2* in HSCs effectively ameliorates liver fibrosis, inflammation, and steatosis in mouse models of fibrosis and MASH via inhibition of TLR4-TGF-β/FAK signaling-mediated HSC activation. Given that the AAV6 serotype possesses a higher transduction efficiency in fibroblasts,[39] relevant myofibroblast tropism, higher safety, lower immunogenicity and greater long-term efficacy in regulating gene expression, we speculate that the AAV6-sh*Thbs2* delivery system represents a promising strategy for the treatment of liver fibrosis that warrants further study.

Abbreviations

AAV6, adeno-associated virus serotype 6; ALT, alanine aminotransferase; αSMA, α-smooth muscle actin; CCl_4, carbon tetrachloride; CMV, cytomegalovirus; ECM, extracellular matrix; FAK, focal adhesion kinase; HSC, hepatic stellate cell; MASH, metabolic dysfunction-associated steatohepatitis; MCD, methionine-choline deficient; shRNA, short-hairpin RNA; TGF-β, transforming growth factor beta; THBS2, thrombospondin 2; TLR4, toll-like receptor 4.

Financial support

This work was supported by the National Natural Science Foundation of China (82000570 [to X.W.], 81970524 [to H.Y.], 82130018 [to H.Y.], 82170613 [to W.C.], 81800534 [to W.C.]), National Science and Technology Major Project (2018ZX10302204) (to H.Y.), and Beijing Municipal Science & Technology Commission (Z22110000742215 [to Y.S.]).

Conflict of interest

The authors of this study declare that they do not have any conflict of interest.

Please refer to the accompanying ICMJE disclosure forms for further details.

Authors' contributions

HY, WC and XW contributed to the conception and design; HY supervised this study; NZ performed all the experiments with the supports from WC, WZ, XY, AX, QH and AY; NZ analyzed and interpreted the data with the supports of WC, WZ, YS and HY; WC and NZ drafted the manuscript; HY, XW, WC and YS funded this study; HY and XW critically revised this manuscript. All authors reviewed and edited this manuscript.

Data availability statement

All reagents, antibodies and resources used in this research can be found in the CTAT table.

Supplementary data

Supplementary data to this article can be found online at https://doi.org/10.1016/j.jhepr.2024.101014.

References

Author names in bold designate shared co-first authorship

[1] Higashi T, Friedman SL, Hoshida Y. Hepatic stellate cells as key target in liver fibrosis. Adv Drug Deliv Rev 2017;121:27–42.
[2] Vento S, Cainelli F. Chronic liver diseases must be reduced worldwide: it is time to act. Lancet Glob Health 2022;10:e471–e472.
[3] Marcellin P, Gane E, Buti M, et al. Regression of cirrhosis during treatment with tenofovir disoproxil fumarate for chronic hepatitis B: a 5-year open-label follow-up study. Lancet 2013;381:468–475.
[4] Vilar-Gomez E, Martinez-Perez Y, Calzadilla-Bertot L, et al. Weight loss through lifestyle modification significantly reduces features of nonalcoholic steatohepatitis. Gastroenterology 2015;149:367–378. e365; quiz e314-365.
[5] Sun Y, Zhou J, Wang L, et al. New classification of liver biopsy assessment for fibrosis in chronic hepatitis B patients before and after treatment. Hepatology 2017;65:1438–1450.
[6] Xu C, Yan L, Guan X, et al. Tsp2 facilitates tumor-associated fibroblasts formation and promotes tumor progression in retroperitoneal liposarcoma. Int J Biol Sci 2022;18:5038–5055.
[7] **Yang H**, **Sun B**, **Fan L**, et al. Multi-scale integrative analyses identify THBS2(+) cancer-associated fibroblasts as a key orchestrator promoting aggressiveness in early-stage lung adenocarcinoma. Theranostics 2022;12:3104–3130.
[8] Nan P, Dong X, Bai X, et al. Tumor-stroma TGF-beta1-THBS2 feedback circuit drives pancreatic ductal adenocarcinoma progression via integrin alpha(v)beta(3)/CD36-mediated activation of the MAPK pathway. Cancer Lett 2022;528:59–75.
[9] Carpino G, Cardinale V, Di Giamberardino A, et al. Thrombospondin 1 and 2 along with PEDF inhibit angiogenesis and promote lymphangiogenesis in intrahepatic cholangiocarcinoma. J Hepatol 2021;75:1377–1386.
[10] Tarao K, Nozaki A, Ikeda T, et al. Real impact of liver cirrhosis on the development of hepatocellular carcinoma in various liver diseases-meta-analytic assessment. Cancer Med 2019;8:1054–1065.
[11] **Pantano L**, **Agyapong G**, **Shen Y**, et al. Molecular characterization and cell type composition deconvolution of fibrosis in NAFLD. Sci Rep 2021;11:18045.
[12] **Chen W**, **Wu X**, Yan X, et al. Multitranscriptome analyses reveal prioritized genes specifically associated with liver fibrosis progression independent of etiology. Am J Physiol Gastrointest Liver Physiol 2019;316:G744–g754.
[13] **Kozumi K**, **Kodama T**, Murai H, et al. Transcriptomics identify thrombospondin-2 as a biomarker for NASH and advanced liver fibrosis. Hepatology 2021;74:2452–2466.
[14] Iwadare T, Kimura T, Tanaka N, et al. Circulating thrombospondin 2 levels reflect fibrosis severity and disease activity in HCV-infected patients. Sci Rep 2022;12:18900.
[15] Calabro NE, Barrett A, Chamorro-Jorganes A, et al. Thrombospondin-2 regulates extracellular matrix production, LOX levels, and cross-linking via downregulation of miR-29. Matrix Biol 2019;82:71–85.

between NC$^{\alpha SMA\text{-}Pr}$ and sh$^{\alpha SMA\text{-}Pr}$ mice fed the MCD diet. (K) Immunoblotting analyses and comparisons of THBS2, COL-1, αSMA, TLR4, p-FAK, FAK, p-SMAD2, and SMAD2 protein expression between NC$^{\alpha SMA\text{-}Pr}$ and sh$^{\alpha SMA\text{-}Pr}$ mice fed the MCD diet. Data are presented as the mean ± SEM (n = 5/group). Statistical evaluation was performed using Student's *t* test (*p <0.05; **p <0.01, ***p <0.001, ****p <0.0001). AAV6, adeno-associated virus serotype 6; ALT, alanine aminotransferase; AST, aspartate aminotransferase; CPA, collagen proportionate area; EGFP, enhanced GFP; HSCs, hepatic stellate cells; IPGTT, intraperitoneal glucose tolerance test; MCD, methionine-choline deficient; n.s., not significant; SR, Sirius red; TC, total cholesterol; TG, triglyceride.

[16] Kyriakides TR, Zhu YH, Smith LT, et al. Mice that lack thrombospondin 2 display connective tissue abnormalities that are associated with disordered collagen fibrillogenesis, an increased vascular density, and a bleeding diathesis. J Cel Biol 1998;140:419–430.
[17] Chen W, Yan X, Xu A, et al. Dynamics of elastin in liver fibrosis: accumulates late during progression and degrades slowly in regression. J Cel Physiol 2019;234:22613–22622.
[18] Ramachandran P, Dobie R, Wilson-Kanamori JR, et al. Resolving the fibrotic niche of human liver cirrhosis at single-cell level. Nature 2019;575:512–518.
[19] Rezvani M, Espanol-Suner R, Malato Y, et al. In vivo hepatic reprogramming of myofibroblasts with AAV vectors as a therapeutic strategy for liver fibrosis. Cell Stem Cell 2016;18:809–816.
[20] **Chen H**, **Cai J**, **Wang J**, et al. Targeting Nestin(+) hepatic stellate cells ameliorates liver fibrosis by facilitating TbetaRI degradation. J Hepatol 2021;74:1176–1187.
[21] Luedde T, Schwabe RF. NF-kappaB in the liver–linking injury, fibrosis and hepatocellular carcinoma. Nat Rev Gastroenterol Hepatol 2011;8:108–118.
[22] Fujita T, Narumiya S. Roles of hepatic stellate cells in liver inflammation: a new perspective. Inflamm Regen 2016;36:1.
[23] **Liu JF**, **Lee CW**, Tsai MH, et al. Thrombospondin 2 promotes tumor metastasis by inducing matrix metalloproteinase-13 production in lung cancer cells. Biochem Pharmacol 2018;155:537–546.
[24] **Xu C**, **Gu L**, **Kuerbanjiang M**, et al. Thrombospondin 2/toll-like receptor 4 Axis contributes to HIF-1alpha-Derived glycolysis in colorectal cancer. Front Oncol 2020;10:557730.
[25] Seki E, De Minicis S, Osterreicher CH, et al. TLR4 enhances TGF-beta signaling and hepatic fibrosis. Nat Med 2007;13:1324–1332.
[26] Chen X, Zhao Y, Wang X, et al. FAK mediates LPS-induced inflammatory lung injury through interacting TAK1 and activating TAK1-NFkappaB pathway. Cell Death Dis 2022;13:589.
[27] Wu X, Cheung CKY, Ye D, et al. Serum thrombospondin-2 levels are closely associated with the severity of metabolic syndrome and metabolic associated fatty liver disease. J Clin Endocrinol Metab 2022;107:e3230–e3240.
[28] Dewidar B, Meyer C, Dooley S, et al. TGF-beta in hepatic stellate cell activation and liver fibrogenesis-Updated 2019. Cells 2019;vol. 8.
[29] Liu X, Hu H, Yin JQ. Therapeutic strategies against TGF-beta signaling pathway in hepatic fibrosis. Liver Int 2006;26:8–22.
[30] **Chen W**, **Zhao W**, Yang A, et al. Integrated analysis of microRNA and gene expression profiles reveals a functional regulatory module associated with liver fibrosis. Gene 2017;636:87–95.
[31] Zhao XK, Yu L, Cheng ML, et al. Focal adhesion kinase regulates hepatic stellate cell activation and liver fibrosis. Sci Rep 2017;7:4032.
[32] Zhang S, Yang H, Xiang X, et al. THBS2 is closely related to the poor prognosis and immune cell infiltration of gastric cancer. Front Genet 2022;13:803460.
[33] **Meng H**, **Zhang X**, Lee SJ, et al. Low density lipoprotein receptor-related protein-1 (LRP1) regulates thrombospondin-2 (TSP2) enhancement of Notch3 signaling. J Biol Chem 2010;285:23047–23055.
[34] Ablinger C, Geisler SM, Stanika RI, et al. Neuronal alpha(2)delta proteins and brain disorders. Pflugers Arch 2020;472:845–863.
[35] Bu FT, Jia PC, Zhu Y, et al. Emerging therapeutic potential of adeno-associated virus-mediated gene therapy in liver fibrosis. Mol Ther Methods Clin Dev 2022;26:191–206.
[36] Kiourtis C, Wilczynska A, Nixon C, et al. Specificity and off-target effects of AAV8-TBG viral vectors for the manipulation of hepatocellular gene expression in mice. Biol Open 2021;10.
[37] Zhu H, Shan Y, Ge K, et al. Specific overexpression of mitofusin-2 in hepatic stellate cells ameliorates liver fibrosis in mice model. Hum Gene Ther 2020;31:103–109.
[38] Lund PK. The alpha-smooth muscle actin promoter: a useful tool to analyse autocrine and paracrine roles of mesenchymal cells in normal and diseased bowel. Gut 1998;42:320–322.
[39] Crystal RG. Adenovirus: the first effective in vivo gene delivery vector. Hum Gene Ther 2014;25:3–11.